Origin and evolution of carnivorism in the Ascomycota (fungi)

Ence Yang[a,1], Lingling Xu[a,b,1], Ying Yang[a], Xinyu Zhang[a], Meichun Xiang[a], Chengshu Wang[c], Zhiqiang An[d,2], and Xingzhong Liu[a,2]

[a]State Key Laboratory of Mycology, Institute of Microbiology, Chinese Academy of Sciences, Beijing 100101, China; [b]College of Biotechnology, Xi'an University of Arts and Science, Xi'an 710065, China; [c]Key Laboratory of Insect Developmental and Evolutionary Biology, Institute of Plant Physiology and Ecology, Shanghai Institutes for Biological Sciences, Chinese Academy of Sciences, Shanghai 200032, China; and [d]Brown Foundation Institute of Molecular Medicine, University of Texas Health Science Center at Houston, Houston, TX 77030

Edited* by Joan Wennstrom Bennett, Rutgers University, New Brunswick, NJ, and approved May 18, 2012 (received for review December 21, 2011)

Carnivorism is one of the basic life strategies of fungi. Carnivorous fungi possess the ability to trap and digest their preys by sophisticated trapping devices. However, the origin and development of fungal carnivorism remains a gap in evolution biology. In this study, five protein-encoding genes were used to construct the phylogeny of the carnivorous fungi in the phylum Ascomycota; these fungi prey on nematodes by means of specialized trapping structures such as constricting rings and adhesive traps. Our analysis revealed a definitive pattern of evolutionary development for these trapping structures. Molecular clock calibration based on two fossil records revealed that fungal carnivorism diverged from saprophytism about 419 Mya, which was after the origin of nematodes about 550–600 Mya. Active carnivorism (fungi with constricting rings) and passive carnivorism (fungi with adhesive traps) diverged from each other around 246 Mya, shortly after the occurrence of the Permian–Triassic extinction event about 251.4 Mya. The major adhesive traps evolved around 198–208 Mya, which was within the time frame of the Triassic–Jurassic extinction event about 201.4 Mya. However, no major carnivorous ascomycetes divergence was correlated to the Cretaceous–Tertiary extinction event, which occurred more recently (about 65.5 Mya). Therefore, a causal relationship between mass extinction events and fungal carnivorism evolution is not validated in this study. More evidence including additional fossil records is needed to establish if fungal carnivorism evolution was a response to mass extinction events.

As major decomposers, fungi play a critical role in degrading organic matter to inorganic molecules in most ecosystems (1). The majority of fungi adopted saprophytic or symbiotic (including parasitic) lifestyles (2). However, a small portion (less than 0.5%) in the kingdom Fungi are carnivorous and possess the ability to trap and digest nematodes, rhizopods, and rotifers by specialized trapping devices (3–6). Carnivorous fungi, which capture prey by trophic cells, contain species within the phyla Zygomycota (Zoopagaceae), Basidiomycota (*Nematoctonus*), and Ascomycota (Orbiliomycetes) (7, 8). Carnivorous fungi in the Zygomycota produce adhesive hyphae or hyphal protuberances that passively capture small animals (9); little is known about the biology and evolution of those fungi because they cannot be cultured on artificial media (10). Carnivorous fungi in the Basidiomycota produce special adhesive knobs or adhesive spores to capture victims (11, 12). All carnivorous fungi in the Basidiomycota belong to *Nematoctonus*, an anamorphic genus of *Hohenbuehelia* (Pleurotaceae family) that produces gilled mushrooms (13, 14). *Nematoctonus* spp. evolved from an ancestor in *Pleurotus* that produced nematode-toxic droplets (15). More than 90% of the carnivorous fungi belong to the Orbiliomycetes in the Ascomycota (7), where they form a monophylogenetic group (16, 17). To capture nematodes and other prey, carnivorous fungi in the Ascomycota produce sophisticated trapping structures, including one type of active mechanical trap (constricting rings, CR) and five types of passive adhesive traps: sessile adhesive knobs (SSK), stalked adhesive knobs (SK), adhesive nets (AN), adhesive columns (AC), and nonconstricting rings (NCR). Nonconstricting rings are always associated with stalked adhesive knobs and are referred to as NCR + SK in this study (18, 19).

In part because carnivory is rare among fungi, researchers have speculated on how such unusual behavior evolved. One hypothesis is that carnivory was selected for in environments where dead wood and soil are rich in carbon but poor in nitrogen. In nitrogen-poor environments, direct capture of nitrogen from small animals would give carnivorous fungi a competitive advantage over strictly saprophytic fungi (20). However, this hypothesis does not explain why carnivorous fungi are not more abundant and widespread in many environmental niches where small animal prey are readily available. In most environments where saprophytic fungi flourish, it seems likely that the expenditure of nutrients and energy for producing trapping devices may reduce the competitiveness of carnivorous fungi, as producing traps costs additional energy in carnivorous plants (21). A problem with this hypothesis is that, unlike the symbiotic fungi, which independently evolved from saprophytic fungi many times (22), carnivorous fungi evidently evolved from saprophytic fungi only a few times, as indicated by their close clustering in three phyla (Fig. S1). If the key to the development of fungal carnivory is the presence of a carbon-rich, nitrogen-poor environment, one would expect that carnivory have arisen many times. Moreover, degeneration of carnivorous ability seems to characterize the evolution of these fungi (15). These intriguing questions surrounding the origin and evolution of fungal carnivorism remain unsolved.

Estimating when carnivorous fungi diverged from other fungi has been difficult due to the lack of fossil records (23). With the recent discovery of fossils that provide multiple calibration points (24–27), however, it is now possible to more accurately estimate the divergence times of carnivorism in the Ascomycota, in which the diversity of both species and trapping structures is much higher than in the other two carnivorous fungal groups.

Author contributions: Z.A. and X.L. designed research; L.X., Y.Y., and M.X. performed research; E.Y., L.X., and Y.Y. contributed new reagents/analytic tools; E.Y., L.X., X.Z., C.W., Z.A., and X.L. analyzed data; and E.Y., Z.A., and X.L. wrote the paper.

The authors declare no conflict of interest.

*This Direct Submission article had a prearranged editor.

Data deposition: The sequences reported in this paper have been deposited in the GenBank database (accession nos. AY773365, AY773366, AY773368, AY773370, AY773372, AY773374, AY773375, AY773380-AY773385, AY773395, AY773396, AY773398, AY773400, AY773402, AY773404, AY773405, AY773409-AY773414, AY773424, AY773425, AY773427, AY773429, AY773431, AY773433, AY773434, AY773438-AY773443, AY965822, DQ358227, DQ358229, DQ999800, DQ999810, DQ999840, DQ999851, DQ999861, DQ999867, FJ687350, FJ687352-FJ687361, FJ687363-FJ687366, FJ687368, FJ687370-FJ687379, FJ687381-FJ687384, JX124391, and JX124392).

[1]E.Y. and L.X. contributed equally to this work.

[2]To whom correspondence may be addressed. E-mail: zhiqiang.an@uth.tmc.edu or liuxz@im.ac.cn.

This article contains supporting information online at www.pnas.org/lookup/suppl/doi:10.1073/pnas.1120915109/-/DCSupplemental.

The evolution of ascomycetes that prey on nematodes was found to have evolved along two lineages: that of fungi that capture prey by constricting rings and that of fungi that capture prey by adhesive structures (16).

In the present study, we investigated the origin of carnivorism in the Ascomycota by three approaches. First, we conducted a phylogenetic analysis based on five protein-coding genes from 16 carnivorous species in the Ascomycota representing a broad diversity of trapping structures. Second, we used two fossil records of carnivorous fungi in the Ascomycota as calibration points to estimate when these fungi originated and diverged (24–26). Third, we estimated when carnivorism diverged from saprophytism in the Ascomycota by using the genome information of *Drechslerella stenobrocha*, which produces constricting rings.

Results

Evolution of the Carnivorous Structures in Ascomycota. Various hypotheses on the evolution of trapping structures in the Ascomycota have been proposed, but conflicts exist between molecular (28–30) and phenotypic (7, 31) phylogenies. We have reported that the initial trapping structure evolved along two lineages yielding two distinct trapping mechanisms—the constricting rings and the adhesive traps—but the evolution of the adhesive traps is still ambiguous, partly because the number of taxa representing each type of trapping device was uneven (there were more taxa with adhesive networks than with other adhesive devices) (16). In the current study, we selected 16 taxa representing the six trapping structures: three species each for constricting rings, sessile adhesive knobs, and adhesive nets; three isolates within one species of adhesive columns; and two species each for stalked adhesive knobs and nonconstricting rings (Table 1). As expected, individual nuclear genes did not provide a robust analysis because of limited informative content (Fig. S2). However, the Bayesian inference phylogenetic tree, which was constructed with a data set consisting of 2,289 bp from five genes and with a partitioned strategy, yielded a clear hypothesis regarding the evolution of carnivorous fungi in Ascomycota (Fig. 1). To minimize bias of the combined gene sequences, we constructed phylogenetic trees by varying the order of the combined gene sequences, and the same topology was obtained for the four trees (Fig. S3). Taxa with the same trapping structure clustered together in the resulting consensus phylogenetic tree (Fig. 1 and Fig. S3). The topology was also tested by a 1,000 bootstrap maximum-likelihood analysis, and the bootstrap values for most of the major clades were higher than 80%, except one clade between stalked adhesive knobs and nonconstricting rings that is weakly supported by a bootstrap value of 53% (Fig. 1 and Fig. S4). The results suggest that the evolutionary relationship between SK and NCR + SK is not fully resolved. One explanation is that the SKs are still in the process of diverging from the NCR + SK.

The phylogenetic tree resulting from the five combined nuclear genes not only confirmed our previous results of predicting evolutionary trends of predacious cells in the Ascomycota (16), but also provided insight into the evolution of the adhesive trapping device lineage. The new tree resolved the adhesive lineage into two major groups: one included the SSKs and AC clades, and the other included the ANs, SKs, and NCR + SK clades (Fig. 1 and Fig. S3). The high Bayesian posterior probabilities supported the monophyly of the AC clade and the monophyly of the group including the SSK clade and AC clade, suggesting that ACs were derived from SSKs. In the other lineage, the divergence among ANs, SK and nonconstricting rings plus stalked adhesive knobs (NCR + SK) is not fully resolved in Fig. 1. However, SKs might have derived from ANs and NCR + SK if *Tuber melanosporum* is added as an outgroup (Fig. 2).

Estimation of the Divergence Times of Carnivorous Structures in Ascomycota. Times of origination and divergence of the carnivorous structures were estimated by the combined gene sets. The divergence time estimation may be unreliably relaxed if the root range is unlimited. *T. melanosporum* (Pezizomycetes), whose genome sequence has been published (32), was used as an outgroup because the base of Pezizomycetes and Orbiliomycetes represents the crown of Pezizomycotina (33, 34). The root calibration was set around 300–500 Mya (23). Two fossil records were also included in the calibration (24–26). One of the fossils was identified as an extinct trapping structure (unicellular ring, or UCR) that was ancestral to ANs and NCRs (26) and was

Table 1. GenBank accession numbers for sequences used in the phylogenetic analysis of carnivorous Ascomycota

Species	Trapping structure*	Isolate	*bt* (240 bp)† SYM + G‡	*ef* (444 bp)† GTR + G‡	*rpb2* (717 bp)† SYM + I + G‡	*mapk* (345 bp)† GTR + I + G‡	*sp* (543 bp)† SYM + I + G‡
Arthrobotrys musiformis	AN1	SQ77-1	AY773382	AY773411	AY773440	FJ687361	FJ687379
A. oligospora	AN2	920	AY773374	AY773404	AY773433	FJ687359	FJ687377
A. vermicola	AN3	629	AY773366	AY773396	AY773425	FJ687360	FJ687378
Dactylellina appendiculata	SK + NCR1	CBS206.64	AY965822	DQ358227	DQ358229	FJ687364	FJ687382
Da. drechsleri	SK1	CBS546.63	DQ999861	DQ999840	DQ999810	FJ687366	FJ687384
Da. ellipsospora	SK2	YNWS02-8–1	*AY773370*	AY773400	AY773429	FJ687365	FJ687383
Da. haptotyla	SK + NCR2	CBS113354	AY773383	AY773412	AY773441	FJ687363	FJ687381
Drechslerella brochopaga	CR1	701	AY773368	AY773398	AY773427	FJ687350	FJ687368
Dr. dactyloides	CR2	Expo-5	AY773375	AY773405	AY773434	FJ687352	FJ687370
Dr. stenobrocha	CR3	YNWS02-9–1	AY773372	AY773402	AY773431	JX124391	JX124392
Gamsylella cionopaga	AC1	SQ27-3	AY773380	AY773409	AY773438	FJ687354	FJ687372
G. cionopaga	AC2	SQ60-2	AY773381	AY773410	AY773439	FJ687353	FJ687371
G. cionopaga	AC3	XJ03-136–1	AY773384	AY773413	AY773442	FJ687355	FJ687373
G. querci	SSK1	4173	AY773365	AY773395	AY773424	FJ687358	FJ687376
G. robusta	SSK2	CBS110125	DQ999867	DQ999851	DQ999800	FJ687357	FJ687375
G. parvicollis	SSK3	XJ03-52–1	AY773385	AY773414	AY773443	FJ687356	FJ687374

*AC, adhesive column; AN, adhesive net; CR, constricting ring; NCR, nonconstricting ring; OUT, outgroup; SSK, sessile adhesive knob; SK, stalked adhesive knob.

†*bt*, β-tubulin; *ef*, elongation factor 1-α; *mapk*, mitogen-activated protein kinase; *rpb2*, RNA polymerase subunit II; *sp*, subtilisin-like serine protease.

‡Best nucleotide substitution model for each gene. SYM, symmetrical model; G, gamma distribution; GTR, general time reversible; I, proportion of invariable sites.

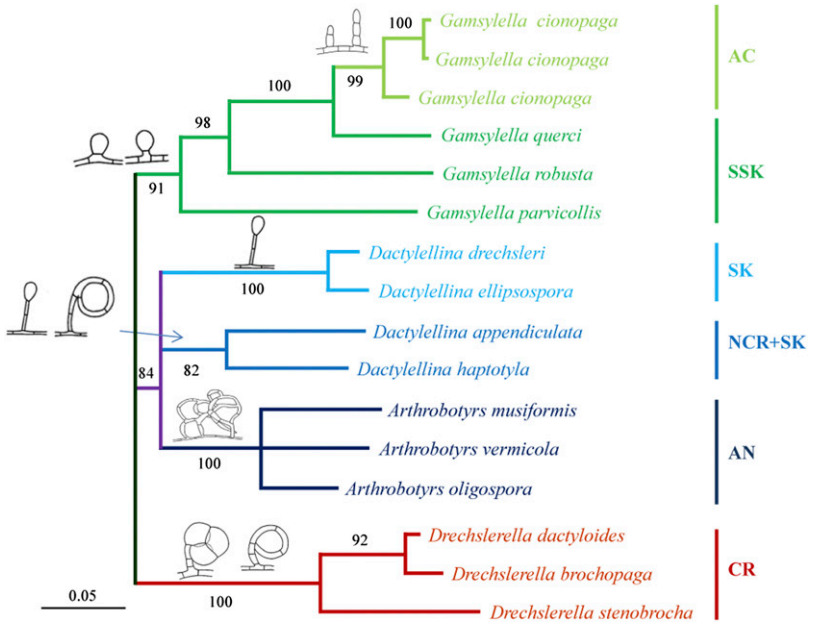

Fig. 1. Bayesian-inferred phylogenetic tree of carnivorous Orbiliomycetes by five protein-coding genes. The tree was constructed by MrBayes with a portioned strategy. All associated parameters were unlinked. The topology was also tested by a 1,000 bootstrap maximum-likelihood analysis; the bootstrap value is marked on the branch. The branches with a bootstrap value lower than 70% are not shown. Trapping devices are drawn on the left. SSK, sessile adhesive knob; SK, stalked adhesive knob; AN, adhesive net; AC, adhesive column; NCR, nonconstricting ring; CR, constricting ring.

dated to 100 Mya (26). This fossil record enabled us to estimate the divergence time of the last common ancestor (LCA) of ANs and NCRs (Fig. 2, node A). The limits to node A were from 100 Mya (fossil) (25, 26) to 500 Mya (crown of Pezizomycotina) (23). The second fossil record contained SKs and was dated to about 22.5–26 Mya (24), and this fossil record enabled us to estimate the divergence time of the LCA of SKs (Fig. 2, node B). The limits to node B were from 24 Mya (fossil) (24) to 500 Mya (crown of Pezizomycotina) (23).

With these calibrations, we estimated that the divergence times of major evolutionary events in carnivorous ascomycetes and Pezizomycotina diverged about 419 Mya (95% highest posterior density (HPD: 316–500 Mya). It took more than 150 million years for the carnivorous fungi to further diverge, and the LCA for carnivorous fungi in the Ascomycota centered on 246 Mya (95% HPD: 158–349 Mya). The LCA of the mechanic trapping device (constricting rings) and the adhesive trapping structures (adhesive columns, adhesive nets, nonconstricting rings, stalked adhesive knobs, and sessile adhesive knobs) centered on 148 Mya (95% HPD: 82–229 Mya) and 208 Mya (95% HPD: 138–303 Mya), respectively. Within the adhesive trapping devices, the SSKs and ACs originated 198 Mya (95% HPD: 125–286 Mya)

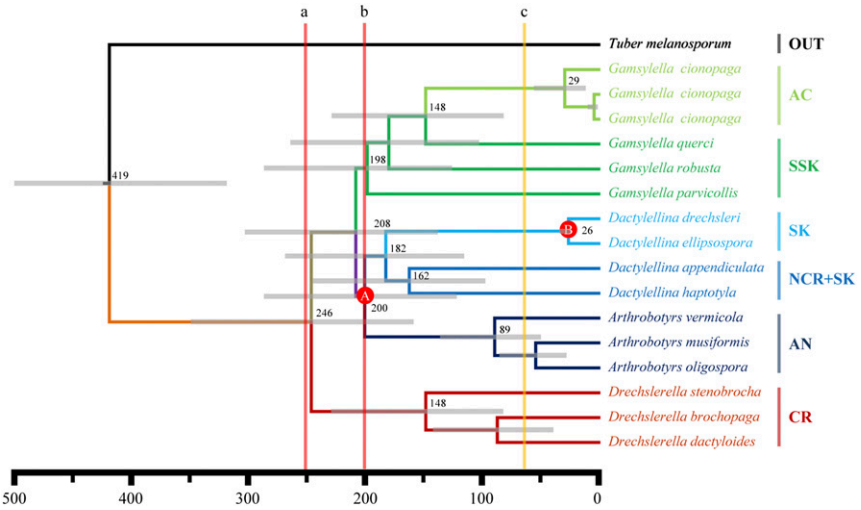

Fig. 2. Estimated divergence times of the major lineages in the carnivorous Orbiliomycetes. Chronogram was constructed using BEAST based on the Bayesian-inferred tree with three calibrations: root node (300–500 Mya), node A (100–500 Mya), and node B (24–500 Mya). Deep-branching phylogeny illustrating the relationships among different lineages is shown by different colors. Error bars are shown and each represents the 95% highest posterior density (HPD) for a node age. The red lines "a" and "b" represent the mass extinction events of the Permian–Triassic (251.4 Mya) and the Triassic–Jurassic (201.4 Mya), respectively. The orange line "c" represents the mass extinction event of the Cretaceous–Tertiary (65.5 Mya). Nodes A and B indicate the two fossil calibration nodes. SSK, sessile adhesive knob; SK, stalked adhesive knob; AN, adhesive net; AC, adhesive column; NCR, nonconstricting ring; CR, constricting ring.

and differentiated adhesive columns 29 Mya (95% HPD: 11–55 Mya), respectively. The ANs, SKs, and nonconstricting rings originated 200 Mya (95% HPD: 122–286 Mya) and differentiated into adhesive nets 89 Mya (95% HPD: 49–136 Mya), NCR + SK 182 Mya (95% HPD: 115–268 Mya), stalked adhesive knobs 26 Mya (95% HPD: 24–34 Mya), and nonconstricting rings 162 Mya (95% HPD: 97–245 Mya) (Table 2).

Divergence Time for the Pezizomycotina Crown by Phylogenomic Analysis. In the analysis described in Fig. 2, the root node represents the origin of Pezizomycotina around 419 Mya (95% HPD: 316–500 Mya). With genome sequences of *D. stenobrocha*, which possesses CRs and seven other fungal genomes (Table S1), we estimated divergence time for the Pezizomycotina crown at three additional calibrated points independent of the two fossil calibrations described in Fig. 2. On the basis of different identifications of taxonomy of a fossil record of *Paleopyrenomycites devonicus*, the divergence time of Ascomycota and Basidiomycota was estimated to be 452, 843, and 1,489 Mya, respectively (23). Therefore, we set the origin of Dikaryotes between 452 and 1,489 Mya. The divergence times of Hypocreales, estimated by the oldest fossil evidence of animals parasitized by fungi, were also verified (23, 27), including the divergence time between Clavicipitaceae and Hypocreaceae around 146–216 Mya and among Nectriaceae, Clavicipitaceae, and Hypocreaceae around 150–213 Mya. The amino acid sequences of *D. stenobrocha* and *Trichoderma reesei* were predicted by Augustus and Genemark, and the predicted proteins were confirmed (35–38). For the six other genomes, we collected the protein sequences on the basis of previous annotations (32, 39–43). Calibration constraints used in the phylogenomic dating analysis are summarized in Table S2.

The basal group of Pezizomycotina is ambiguous to date. One study suggests that Orbiliomycetes is the basal group of Pezizomycotina and that Pezizomycetes diverged afterward (33). The other study proposes that Pezizomycetes is the basal group and that Orbiliomycetes diverged afterward (34). On the basis of the two conflicting hypotheses, we estimated the divergence time of Pezizomycotina with two alternative topologies (Fig. 3 *A* and *B*). We applied the same calibrations to the two topologies: root was set around 452–1,489 Mya; the LCA of Clavicipitaceae and Hypocreaceae (Hypocreales, Sordariomycetes) was centered on 150–213 Mya (27); and the LCA of Nectriaceae, Clavicipitaceae, and Hypocreaceae (Hypocreales, Sordariomycetes) was centered on 146–206 Mya (27). We identified 1,367 orthologous genes from the eight genomes by Inparanoid 4.0 (44). However, 298 genes were excluded from analysis because they failed to apply to at least one topology. Each gene was run in 600,000 generations with tree collecting at every 100th generation. After discarding the first 5,001 sampled trees, 1,000 trees remained for each gene. We summarized 1,069,000 trees collected from the 1,069 genes for each topology, and the results showed that time estimation was similar in the two alternative topologies (Fig. 3 *A* and *B*). The divergence time of Pezizomycotina was estimated at 261 Mya (Fig. 3*A*, 95% HPD: 151–525 Mya) and 260 Mya (Fig. 3*B*, 95% HPD: 151–511 Mya) in the alternative topologies. In Fig. 2, we set the upper boundary of Pezizomycotina crown at 500 Mya, and this is reasonable considering the upper ranges of 95% HPD in Fig. 3 *A* and *B* are 525 and 511 Mya, respectively.

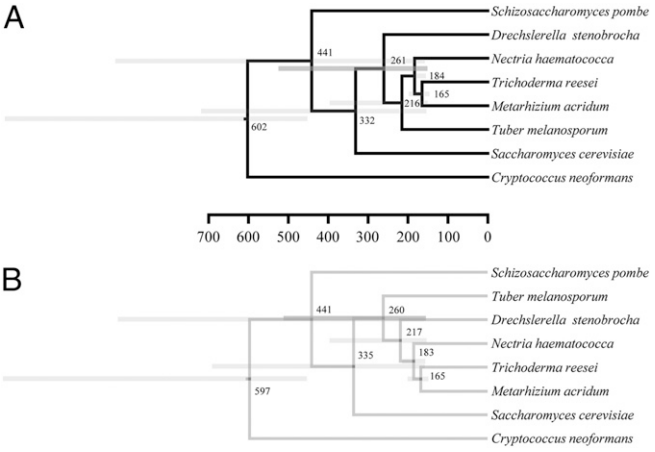

Fig. 3. The origin time of Pezizomycotina with 1,069 orthologs. Three calibrations were applied to the two alternative topologies. The root node was calibrated between 452 and 1,489 Mya. The last common ancestor (LCA) of Nectriaceae, Clavicipitaceae, and Hypocreaceae was calibrated between 150 and 213 Mya. The divergence of Clavicipitaceae and Hypocreaceae was calibrated between 146 and 206 Mya. Error bars are shown, each representing the 95% highest posterior density (95% HPD) for a node age. Geological times are provided on the median axis. SSK, sessile adhesive knob; SK, stalked adhesive knob; AN, adhesive net; AC, adhesive column; NCR, nonconstricting ring; CR, constricting ring. (*A*) Orbiliomycetes is used as the basal group of Pezizomycotima with Pezizomycetes diverging afterward. (*B*) Pezizomycetes is used as the basal group with Orbiliomycetes diverging afterward.

Discussion

Evolution of Carnivorism in the Ascomycota. The differentiation between trapping structures among major clades demonstrated a clear evolutionary path of carnivorous fungi in the Ascomycota. Carnivorous fungi with an active trapping structure (the constricting

Table 2. Divergence time estimation of major clades of carnivorous Ascomycota

Taxa	Node specification		Divergence time (Mya)	95% HPD range (Mya)
	Species 1	Species 2		
Pezizomycotina	*Tuber melanosporum*	*Drechslerella brochopaga*	419	316–500
Carnivorous crown	*Gamsylella parvicollis*	*Dr. brochopaga*	246	158–349
Ancestor of adhesive traps	*G. parvicollis*	*Dactylellina drechsleri*	208	138–303
Ancestor of CR	*Dr. stenobrocha*	*Dr. brochopaga*	148	82–229
Ancestor of NCR	*Da. haptotyla*	*Da. appendiculata*	162	97–245
Ancestor of SK	*Da. ellipsospora*	*Da. drechsleri*	26	24–34
Ancestor of NCR and SK	*Da. haptotyla*	*Da. drechsleri*	182	115–268
Ancestor of AN	*Arthrobotrys vermicola*	*A. oligospora*	89	49–136
Unicell ring (extinct)	*A. vermicola*	*Da. drechsleri*	200	122–286
Ancestor of SSK	*G. parvicollis*	*G. querci*	198	125–286
Ancestor of AC	*G. cionopaga*	*G. cionopaga*	29	11–55

AC, adhesive column; AN, adhesive net; CR, constricting ring; NCR, nonconstricting ring; OUT, outgroup; SK, stalked adhesive knob; SSK, sessile adhesive knob.

EVOLUTION

ring) and those with a passive, adhesive trapping structure split from an unknown ancestor. SSKs and UCRs originated from the adhesive ancestor. ACs diverged from SSKs by the proliferation of adhesive knobs into a column, which increased the adhesive surface and predatory efficiency. the UCR probably became extinct due to low predatory efficiency (the unicellular ring is morphologically similar to NCRs, which have the lowest predatory efficiency of existing trapping fungi). The unicellular ring evolved along two lineages to increase predatory efficiency. One formed ANs by proliferating the ring into a network of rings. The other formed NCRs accompanied by SKs, in which the single-celled rings developed into three-celled nonconstricting rings, unicellular knobs, and SKs. Our results suggest two potential evolutionary relationships between SK and NCR + SK. One possibility is that NCRs were added in some species with stalked adhesive knobs to increase carnivorous efficiency. The other possibility is that fungi with NCR + SK gradually degenerated into species with stalked adhesive knobs only to reduce the high energy cost of producing nonconstricting rings. In our previous study, we hypothesized that the evolutionary trend of carnivorous fungi in Orbiliomycetes (Ascomycota) is toward elongation of the stalk of trapping devices (16). The results from this study not only confirmed that hypothesis, but also demonstrated that the evolutionary trend of carnivorous Orbiliomycetes is toward increased adhesive surface area or elongation of the adhesive structures from the mycelium.

Origin of Fungal Carnivorism in the Orbiliomycetes. It is natural to hypothesize that the nematode-trapping fungi evolved after the appearance of nematodes. The phylum Nematoda and other major invertebrate clades have been proposed to appear during the Cambrian Explosion about 550–600 Mya (45), which is about 130–180 million years ahead of the divergence of carnivorous ascomycetes about 419 Mya as proposed in this study. Fossil records also support the notion that nematodes evolved ahead of carnivorous fungi. One of the nematode fossils dated 396–416 Mya (46), but the oldest carnivorous fungal fossil is dated about 100 Mya (26).

To shed light on the origin of fungal carnivorism, important biological and geological events around the divergence times of the trapping structures were surveyed. Although the 95% HPD range of each node spans a large range, we found that the median timing of the major evolutionary events of these fungi seemed to coincide with mass extinction events. The crown of these carnivorous species arose around 246 Mya, which was 5 million years (Myr) after the Permian–Triassic extinction (251.4 Mya) (47). Major clades of the extant carnivorous species diverged around 208, 200, and 198 Mya, which centered on the Triassic–Jurassic extinction (201.4 Mya).

Mass extinctions resulted in a sharp decrease in the diversity and abundance of macroscopic creatures and the deposition of a huge biomass of dead plants and animals. The dead organic materials supported a significant increase in the diversity and biomass of microorganisms (48). When ecosystems began to recover, these decomposers likely encountered substantial competition for nutrients because most of the dead organic materials had been consumed. Geochronologic and biostratigraphic constraints based on high-precision U-Pb dates of single zircons from south China allow us to place the Early to Middle Triassic (Olenekian–Anisian) boundary at 247.2 Mya (49). The new dates constrain the Early Triassic interval characterized by delayed biotic recovery and carbon-cycle instability to 5 Mya (49). This time constraint must be considered in any model for the end-Permian extinction and subsequent recovery (50). Our data are consistent with a long recovery time in that the crown of extant carnivorous Ascomycota arose about 5 Myr later than the Permian–Triassic extinction event.

In addition to the Permian–Triassic and Triassic–Jurassic extinction events, another extinction event known as the Cretaceous–Tertiary extinction occurred more recently, about 65.5 Mya (51). In the current study, we did not find a similar relationship between carnivorous ascomycetes and the Cretaceous–Tertiary extinction. As our data did not provide tight time estimation for each of the major notes, the relationship between fungal carnivorism evolution and a mass extinction event is not validated in this study. More evidence, including additional fossil records, is needed to establish if fungal carnivorism evolution was a response to mass extinction events.

Materials and Methods

Fungal Isolates and Sequence Collection. Sixteen isolates of carnivorous ascomycetes were used in this study (Table 1). Each of the six trapping structures was represented by three isolates, except the stalked adhesive knobs and nonconstricting rings, which were represented by two isolates. Stalked adhesive knobs occurred without nonconstricting rings in two cases and with nonconstricting rings in two other cases; nonconstricting rings always occurred with stalked adhesive knobs as nonconstricting rings plus stalked adhesive knobs. In most cases, each isolate was selected from a different species. Only *Gamsylella cionopaga* produced adhesive columns traps; however, we used three isolates of this species.

The sequences of *bt*, *ef*, and *rpb2* were obtained from GenBank and from our previous studies (Table 1), while *mapk* and *sp* were newly sequenced. Primers and PCR conditions used in cloning and sequencing of the *mapk* and *sp* genes are detailed in *SI Materials and Methods*. The five corresponding gene sequences of the outgroup were collected from the genome of *T. melanosporum* by BLAST (v.2.2.25) (52).

Phylogenetic Analysis of Carnivorous Fungi in the Ascomycota. DNA sequences were assembled manually. Exons of the protein-coding genes were annotated on the basis of the RefSeq database. Sequences used in phylogenetic analysis were edited with BioEdit (ver. 7.0.5.3) (53, 54) and aligned with ClustalX (ver. 2.0.12) (55). The protein-coding genes were aligned on the basis of the translated amino acid sequences. The nucleotide substitution models of each gene were selected by MrModeltest (ver. 2.3) (56) based on the corrected Akaike Information Criterion. Bayesian phylogenetic analyses and nodal support estimation are detailed in *SI Materials and Methods*.

Divergence Time Estimation of Carnivorous Structures in the Ascomycota. For the molecular dating analysis of the data set, the Bayesian relaxed molecular clock approach was used as implemented in BEAST (ver. 1.6.1) (57). Two internal calibration points corresponding to the fossil records and evolutionary events were used in the analysis as soft constraints following a uniform limitation. These dates corresponded to the formation of stalked adhesive knobs (24–500 Mya) and of unicellular rings (100–500 Mya). The root node, which represented the rise of Pezizomycotina, was set at 300–500 Mya (23). We used as priors the uncorrelated log-normal molecular clock model with a Yule process for the model of speciation, whereas the SR06 model was used for protein-coding genes to describe the nucleotide substitution model. The Markov Chain Monte Carlo calculation is detailed in *SI Materials and Methods*.

Divergence Time Estimation by Phylogenomic Data. We selected eight fungal genomes to verify the root node in Fig. 2 (represented by the divergence between *D. stenobrocha* and *T. melanosporum*) in the Ascomycota (Table 2). Detailed parameters and methods are described in *SI Materials and Methods*.

ACKNOWLEDGMENTS. The authors thank Prof. Bruce A. Jaffee at the University of California for valuable English editing of the manuscript. We also thank the editor and anonymous reviewers. This work was supported by the National Natural Scientific Foundation of China (Grant 30625001) and by The Welch Foundation.

1. Gadd GM (2007) Geomycology: Biogeochemical transformations of rocks, minerals, metals and radionuclides by fungi, bioweathering and bioremediation. *Mycol Res* 111:3–49.
2. Liu XZ, Xiang MC, Che YS (2009) The living strategy of nematophagous fungi. *Mycoscience* 50:20–25.
3. Drechsler C (1941) Four Phycomycetes destructive to nematodes and rhizopods. *Mycologia* 33:248–269.
4. Pramer D (1964) Nematode-trapping fungi. *Science* 144:382–388.
5. Thorn RG, Barron GL (1984) Carnivorous mushrooms. *Science* 224:76–78.

6. McInnes SJ (2003) A predatory fungus (Hyphomycetes: Lecophagus) attacking Rotifera and Tardigrada in maritime Antarctic lakes. *Polar Biol* 26:79–82.
7. Li TF, Zhang KQ, Liu XZ (2000) *Taxonomy of Nematophagous Fungi* (Chinese Scientific and Technological Publications, Beijing).
8. Kirk PM, Cannon PF, Minter DW, Stalpers JA (2008) *Dictionary of the Fungi* (CAB International, Wallingford, Oxon, UK), 10th Ed.
9. Saikawa M (2011) Ultrastructural studies on zygomycotan fungi in the Zoopagaceae and Cochlonemataceae. *Mycoscience* 52:83–90.
10. Duddington CL (1973) Zoopagales. *The Fungi*, eds Ainsworth GC, Sparrow FK, Sussman AS (Academic Press, New York), Vol 4B, pp 231–234.
11. Poloczek E, Webster J (1994) Conidial traps in *Nematoctonus* (nematophagous Basidiomycetes). *Nova Hedwigia* 59:201–205.
12. Durschnerpelz UU (1987) Traps of *Nematoctonus leiosporus*: An unusual feature of an endoparasitic nematophagous fungus. *Trans Br Mycol Soc* 88:129–130.
13. Barron GL, Dierkes Y (1977) Nematophagous fungi: *Hohenbuehelia*, perfect state of *Nematoctonus*. *Can J Bot* 55:3054–3062.
14. Thorn RG, Moncalvo JM, Reddy CA, Vilgalys R (2000) Phylogenetic analyses and the distribution of nematophagy support a monophyletic Pleurotaceae within the polyphyletic pleurotoid-lentinoid fungi. *Mycologia* 92:241–252.
15. Koziak ATE, Cheng KC, Thorn RG (2007) Phylogenetic analyses of *Nematoctonus* and *Hohenbuehelia* (Pleurotaceae). *Can J Bot* 85:762–773.
16. Yang Y, Yang E, An ZQ, Liu XZ (2007) Evolution of nematode-trapping cells of predatory fungi of the Orbiliaceae based on evidence from rRNA-encoding DNA and multiprotein sequences. *Proc Natl Acad Sci USA* 104:8379–8384.
17. Li J, et al. (2010) New insights into the evolution of subtilisin-like serine protease genes in Pezizomycotina. *BMC Evol Biol* 10:68.
18. Barron GL (1977) *The Nematode-Destroyiung Fungi* (Canadian Biological Publications Ltd., Guelph, ON).
19. Stirling GR (1991) *Biological Control of Plant Parasitic Nematodes* (CAB International, Wallingford, UK).
20. Barron GL (2003) Predatory fungi, wood decay, and the carbon cycle. *Biodiversity (Ottawa)* 4(1):3–9.
21. Brewer JS (2003) Why don't carnivorous pitcher plants compete with non-carnivorous plants for nutrients? *Ecology* 84:451–462.
22. Stenroos S, et al. (2010) Multiple origins of symbioses between ascomycetes and bryophytes suggested by a five-gene phylogeny. *Cladistics* 26:281–300.
23. Berbee ML, Taylor JW (2010) Dating the molecular clock in fungi: How close are we? *Fungal Biol Rev* 24:1–16.
24. Jansson HB, Poinar GO (1986) Some possible fossil nematophagous fungi. *Trans Br Mycol Soc* 87:471–474.
25. Schmidt AR, Dörfelt H, Perrichot V (2007) Carnivorous fungi from Cretaceous amber. *Science* 318:1743–1743.
26. Schmidt AR, Dörfelt H, Perrichot V (2008) *Palaeoanellus dimorphus* gen. et sp. nov. (Deuteromycotina): A Cretaceous predatory fungus. *Am J Bot* 95:1328–1334.
27. Sung GH, Poinar GO, Jr., Spatafora JW (2008) The oldest fossil evidence of animal parasitism by fungi supports a Cretaceous diversification of fungal-arthropod symbioses. *Mol Phylogenet Evol* 49:495–502.
28. Liou GY, Tzean SS (1997) Phylogeny of the genus *Arthrobotyrs* and allied nematode-trapping fungi based on rDNA sequences. *Mycologia* 89:876–884.
29. Ahrén D, Ursing BM, Tunlid A (1998) Phylogeny of nematode-trapping fungi based on 18S rDNA sequences. *FEMS Microbiol Lett* 158:179–184.
30. Li Y, et al. (2005) Phylogenetics and evolution of nematode-trapping fungi (Orbiliales) estimated from nuclear and protein coding genes. *Mycologia* 97:1034–1046.
31. Rubner A (1996) Revision of predacious hyphomycetes in the *Dactylella-Monacrosporium* complex. *Stud Mycol* 39:1–129.
32. Martin F, et al. (2010) Périgord black truffle genome uncovers evolutionary origins and mechanisms of symbiosis. *Nature* 464:1033–1038.
33. Spatafora JW, et al. (2006) A five-gene phylogeny of Pezizomycotina. *Mycologia* 98: 1018–1028.
34. Schoch CL, et al. (2009) A class-wide phylogenetic assessment of Dothideomycetes. *Stud Mycol* 64(1):1–15.
35. Stanke M, et al. (2006) AUGUSTUS: Ab initio prediction of alternative transcripts. *Nucleic Acids Res* 34(Web Server issue):W435-W439.
36. Stanke M, Morgenstern B (2005) AUGUSTUS: A web server for gene prediction in eukaryotes that allows user-defined constraints. *Nucleic Acids Res* 33(Web Server issue):W465-W467.
37. Stanke M, Steinkamp R, Waack S, Morgenstern B (2004) AUGUSTUS: A web server for gene finding in eukaryotes. *Nucleic Acids Res* 32(Web Server issue):W309-W312.
38. Besemer J, Borodovsky M (2005) GeneMark: Web software for gene finding in prokaryotes, eukaryotes and viruses. *Nucleic Acids Res* 33(Web Server issue):W451-W454.
39. Wood V, et al. (2002) The genome sequence of *Schizosaccharomyces pombe*. *Nature* 415:871–880.
40. Gao QA, et al. (2011) Genome sequencing and comparative transcriptomics of the model entomopathogenic fungi *Metarhizium anisopliae* and *M. acridum*. *PLoS Genet* 7:e1001264.
41. Coleman JJ, et al. (2009) The genome of *Nectria haematococca*: Contribution of supernumerary chromosomes to gene expansion. *PLoS Genet* 5:e1000618.
42. Goffeau A, et al. (1996) Life with 6000 genes. *Science* 274:546, 563–567.
43. Loftus BJ, et al. (2005) The genome of the basidiomycetous yeast and human pathogen *Cryptococcus neoformans*. *Science* 307:1321–1324.
44. O'Brien KP, Remm M, Sonnhammer ELL (2005) Inparanoid: A comprehensive database of eukaryotic orthologs. *Nucleic Acids Res* 33(Database issue):D476–D480.
45. van Megen H, et al. (2009) A phylogenetic tree of nematodes based on about 1200 full-length small subunit ribosomal DNA sequences. *Nematology* 11:927–950.
46. Poinar G, Kerp H, Hass H (2008) *Palaeonema phyticum* gen. n., sp. n. (Nematoda: Palaeonematidae fam. n.), a Devonian nematode associated with early land plants. *Nematology* 10:9–14.
47. Jin YG, et al. (2000) Pattern of marine mass extinction near the Permian-Triassic boundary in South China. *Science* 289:432–436.
48. Visscher H, et al. (1996) The terminal Paleozoic fungal event: Evidence of terrestrial ecosystem destabilization and collapse. *Proc Natl Acad Sci USA* 93:2155–2158.
49. Wang JA, et al. (2008) Chronology and geochemistry of the volcanic rocks in Woruo Mountain region, northern Qiangtang depression: Implications to the Late Triassic volcanic-sedimentary events. *Sci China Ser D* 51:194–205.
50. Lehrmann DJ, et al. (2006) Timing of recovery from the end-Permian extinction: Geochronologic and biostratigraphic constraints from south China. *Geology* 34: 1053–1056.
51. Schulte P, et al. (2010) The Chicxulub asteroid impact and mass extinction at the Cretaceous-Paleogene boundary. *Science* 327:1214–1218.
52. Altschul SF, et al. (1997) Gapped BLAST and PSI-BLAST: A new generation of protein database search programs. *Nucleic Acids Res* 25:3389–3402.
53. Hall T (2005) *BioEdit: Biological Sequence Alignment Editor for Win95/98/NT/2K/XP*. (Ibis Therapeutics, Carlsbad, CA).
54. Hall TA (1999) BioEdit: A user-friendly biological sequence alignment editor and analysis program for Windows 95/98/NT. *Nucleic Acids Symp Ser* 41:95–98.
55. Larkin MA, et al. (2007) Clustal W and clustal X version 2.0. *Bioinformatics* 23: 2947–2948.
56. Nylander JAA (2004) *MrModeltest v2*. Program distributed by the author (Evolutionary Biology Centre, Uppsala University, Uppsala, Sweden).
57. Drummond AJ, Rambaut A (2007) BEAST: Bayesian evolutionary analysis by sampling trees. *BMC Evol Biol* 7:214.